



32 de Biología, Universidad de Murcia, 30100 Murcia, Spain, ¹⁴Institut des Sciences de l'Evolution de
33 Montpellier, UMR 5554 Université Montpellier 2, Bat.22, CC061, Place Eugène Bataillon, 34095
34 Montpellier Cedex 5, France, ¹⁵Duke Trinity College of Art & Sciences, Durham, NC 27708, USA,
35 ¹⁶UMR 7194 CNRS, Histoire naturelle de l'Homme Préhistorique, Département de Préhistoire,
36 Muséum national d'Histoire naturelle, Paris, France, ¹⁷The York Institute for Tropical Ecosystem
37 Dynamics (KITE), Environment Department, University of York, York, Heslington, YO10 5DD,
38 ¹⁸UK, Department of Zoology, Duke University, Box 90325, Durham, NC 27708–0325 U.S.A.,
39 ¹⁹MARUM—Center for Marine Environmental Sciences, University of Bremen, D-28359 Bremen,
40 Germany, ²⁰Discipline of Geography, School of Agricultural, Earth & Environmental Sciences,
41 University of KwaZulu-Natal, Pietermaritzburg, South Africa, ²¹Quaternary Environments and
42 Geoarchaeology, Geography, School of Environment and Development, University of Manchester,
43 Oxford Road, Manchester M13 9PL, UK, ²²Dipartimento di Biologia Ambientale, Sapienza Università di
44 Roma, Italy, ²³Departamento de Ciencias Biológicas, Universidad de los Andes, A.A. 4976 Bogotá,
45 Colombia, ²⁴Palaeoecology & Landscape Ecology, University of Amsterdam, The Netherlands,
46 ²⁵Geology and Environmental Science Department, Norwich University, VT 05663, USA, ²⁶University
47 of Minnesota, Department of Earth Sciences, Minneapolis, Minnesota 55455, USA, ²⁷Lake Biwa
48 Museum, Oroshimocho1091, Kusatsu 525-0001, Japan, ²⁸Department of Physical Geography and the
49 Bolin Centre for Climate Research, Stockholm University, Stockholm, Sweden, ²⁹Lamont-Doherty
50 Earth Observatory of Columbia University, Palisades, NY 10601, USA, ³⁰Department of Archaeology
51 and Natural History, The Australian National University, Fellows Road, Acton ACT 0200, ³¹Institute for
52 Paleoenvironment of Northern Regions, Koyochō 3-7-5, Kitahiroshima 061-1134, Japan, ³²Geological
53 Institute, University of Tokyo, Hongo, Bunkyo-ku, Tokyo 113-0033, Japan, ³³Roy M. Huffington
54 Department of Earth Sciences, Southern Methodist University, Dallas, TX 75275-0395, USA,
55 ³⁴Departamento de Estratigrafía y Paleontología, Universidad de Granada, 18071, Spain, ³⁵Institute of
56 Mountain Science, Shinshu University, Asahi 3-1-1, Matsumoto 390-8621, Japan, ³⁶School of
57 Geography & Environmental Science, Monash University, Clayton, Vic 3168, Australia, ³⁷Department
58 of Environmental Sciences, Faculty of Science, Shinshu University, Asahi 3-1-1, Matsumoto 390-8621,
59 Japan, ³⁸Department of Geography and Sustainable Development, University of St Andrews, St
60 Andrews, KY16 9AL, UK, ³⁹LOCEAN - Laboratoire d'Océanographie et du Climat : Expérimentations et
61 Approches Numériques, UPMC, Paris, France, ⁴⁰Department of Geosciences, National Taiwan
62 University, 1, Sec. 4, Roosevelt Rd. Taipei 106, Taiwan, ROC, ⁴¹Environmental Change Research
63 Centre, Department of Geography, University College London, London WC1E 6BT, UK, ⁴²Centre for
64 Past Climate Change, Department of Geography and Environmental Science, University of Reading,
65 Reading, UK, ⁴³School of Geography, Planning & Environmental Management, The University of
66 Queensland, St Lucia, Australia, ⁴⁴Freie Universität Berlin, Geological Sciences, Palaeontology Section,
67 Berlin, Germany, ⁴⁵Biodiversity and Climate Research Centre, Senckenberganlage 25, 60325
68 Frankfurt, Germany, ⁴⁶Center of Marine Sciences (CCMAR), Algarve University, Campus de Gambelas,
69 8005-139 Faro, Portugal, ⁴⁷Portuguese Sea and Atmosphere Institute (IPMA), Rua Alfredo
70 Magalhães Ramalho 6, 1495-006 Lisboa, Portugal, ⁴⁸School of Geography, Environment and Earth
71 Sciences, Victoria University of Wellington, PO Box 600, Wellington 6140, New Zealand, ⁴⁹Graduate
72 School of Environmental Earth Science, Hokkaido University, N10-W5 Kita-ku, Sapporo 060-0810,
73 Japan, ⁵⁰Unitat de Botànica, Facultat de Biociències, Universitat Autònoma de Barcelona, 08193
74 Bellaterra, Cerdanyola del Vallès, Spain, ⁵¹C.N.R. – Istituto per la Dinamica dei Processi Ambientali,
75 Laboratorio di Palinologia e Paleocologia, Piazza della Scienza 1, 20126 Milano, Italy, ⁵²Department
76 of Earth Sciences, Palynology and Palaeobotany Section, National Museums of Kenya, P.O. Box



77 40658, Nairobi, 00100, Kenya, ⁵³Department of Plant Sciences, University of the Free State, P.O Box
78 339, Bloemfontein, South Africa, ⁵⁴Graduate School of Life and Environmental Sciences, Kyoto
79 Prefectural University, 1-5 Hangi-cho, Shimogamo, Sakyo-ku, Kyoto 606-8522, Japan, ⁵⁵Department
80 of Geography, University of Exeter, Amory Building, Rennes Drive, Exeter, EX4 4RJ, UK, ⁵⁶Department
81 of Paleoecology and Landscape Ecology, Institute for Biodiversity and Ecosystem Dynamics,
82 Universiteit van Amsterdam, Science Park 904, 1098 XH Amsterdam, The Netherlands, ⁵⁷Department
83 of Biological Sciences, Florida Institute of Technology, Melbourne, FL, USA, ⁵⁸GNS Science 1 Fairway
84 Drive, Avalon PO Box 30-368, Lower Hutt, New Zealand ⁵⁹Department of Earth Sciences, Montana
85 State University, Bozeman, MT 59717, USA, ⁶⁰U.S. Geological Survey, 926A National Center, Reston,
86 VA 20192, USA.

87

88 *Correspondence to:* Maria F. Sanchez Gofii (mf.sanchezgoni@epoc.u-bordeaux1.fr)

89

90 **Abstract**

91 Quaternary records provide an opportunity to examine the nature of the vegetation and fire
92 responses to rapid past climate changes comparable in velocity and magnitude to those expected in
93 the 21st century. The best documented examples of rapid climate change in the past are the warming
94 events associated with the Dansgaard-Oeschger (D-O) cycles during the last glacial period, which
95 were sufficiently large to have had a potential feedback through changes in albedo and greenhouse
96 gas emissions on climate. Previous reconstructions of vegetation and fire changes during the D-O
97 cycles used independently constructed age models, making it difficult to compare the changes
98 between different sites and regions. Here we present the ACER (Abrupt Climate Changes and
99 Environmental Responses) global database which includes 93 pollen records from the last glacial
100 period (73-15 ka) with a temporal resolution better than 1,000 years, 32 of which also provide
101 charcoal records. A harmonized and consistent chronology based on radiometric dating (¹⁴C,
102 ²³⁴U/²³⁰Th, OSL, ⁴⁰Ar/³⁹Ar dated tephra layers) has been constructed for 86 of these records, although
103 in some cases additional information was derived using common control points based on event
104 stratigraphy. The ACER database compiles metadata including geospatial and dating information,
105 pollen and charcoal counts and pollen percentages of the characteristic biomes, and is archived in
106 *Microsoft Access*[™] at <https://doi.org/10.1594/PANGAEA.870867>.



107

108 **1. Introduction**

109 There is considerable concern that the velocity of projected 21st century climate change is
110 too fast to allow terrestrial organisms to migrate to climatically suitable locations for their survival
111 (*Loarie et al., 2009; Burrows et al., 2011; Ordonez et al., 2013; Burrows et al., 2014*). The expected
112 magnitude and velocity of 21st century climate warming is comparable to abrupt climate changes
113 depicted in the geologic records, specifically the extremely rapid warming that occurred multiple
114 times during the last glacial period (Marine Isotope Stages 4 through 2, MIS 4-MIS2, 73,500–14,700
115 calendar years, 73.5–14.7 ka). The estimated increases in Greenland atmospheric temperature were
116 5–16°C [*Capron et al., 2010*] and the duration of the warming events between 10 to 200 years
117 [*Steffensen et al., 2008*]. These events are a component of longer-term millennial-scale climatic
118 variability, a pervasive feature through the Pleistocene [*Weirauch et al., 2008*] which were originally
119 identified from Greenland ice archives [*Dansgaard et al., 1984*] and in North Atlantic Ocean records
120 [*Bond and Lotti, 1995; Heinrich, 1988*] and termed Dansgaard-Oeschger (D-O) cycles and Heinrich
121 events (HE) respectively.

122 D-O events are registered worldwide, although the response to D-O warming events is
123 diverse and regionally specific (see e.g. [*Fletcher et al., 2010; Harrison and Sanchez Goñi, 2010;*
124 *Sanchez Goñi et al., 2008*]) and not a linear response to either the magnitude or the duration of the
125 climate change in Greenland. Given that the magnitude, length and regional expression of the
126 component phases of each of the D-O cycles varies [*Johnsen et al., 1992; Sanchez Goñi et al., 2008*],
127 they provide a suite of case studies that can be used to investigate the impact of abrupt climate
128 change on terrestrial ecosystems.

129 The ACER (Abrupt Climate change and Environmental Responses) project was launched in
130 2008 with the aim of creating a global database of pollen and charcoal records from the last glacial
131 (73 - 15 ka, kyr cal BP) which would allow us to reconstruct the regional vegetation and fire changes
132 in response to glacial millennial-scale variability, and evaluate the simulated regional climates



133 resulting from freshwater changes under glacial conditions. Although there are 232 pollen records
134 covering the last glacial period worldwide, only 93 have sufficient resolution and dating control to
135 show millennial-scale variability [Harrison and Sanchez Goñi, 2010]. It was necessary to re-evaluate
136 and harmonize the chronologies of these individual records to be able to compare patterns of change
137 from different regions. In this paper, we present the ACER pollen and charcoal database, including
138 the methodology used for chronological harmonization and explore the potential of this dataset by
139 comparing two harmonized pollen sequences with other palaeoclimatic records. Such a comparison
140 illustrates the novel opportunities for the spatial analyses of global climate events using this research
141 tool.

142
143

144 **2. Data and methods**

145 **2.1. Compilation of the records**

146 The ACER pollen and charcoal database includes records covering part or all of the last glacial
147 period and with a sampling resolution better than 1,000 years. These records were collected as raw
148 data, through direct contact with researchers or from the freely available European and African
149 Pollen Databases. Four records were digitized from publications using the Grapher™ 12 (Golden
150 Software, LLC) because the original data were either lost (Kalaloch: [Heusser, 1972] and Tagua Tagua
151 [Heusser, 1990]) or are not publicly available (Lac du Bouchet [Reille et al., 1998] and Les Echets [de
152 Beaulieu and Reille, 1984]). These digitized records are available as pollen percentages rather than
153 raw counts. All the records are listed and described in Table S1 (supplementary material).

154

155 **2.2. Harmonization of database chronologies**

156 The chronology of each of the records was originally built as a separate entity. In order to
157 produce harmonized chronologies for the ACER database, decisions had to be made about the types
158 of dates to use, the reference age for modern, the choice of calibration curve, the treatment of
159 radiocarbon age reservoirs, and the software used for age-model construction.



160 Radiometric ages (^{14}C , $^{235}\text{U}/^{230}\text{Th}$, OSL, $^{40}\text{Ar}/^{39}\text{Ar}$) and radiometrically-dated tephtras are
161 given preference in the construction of the age models. The tephtra ages were obtained either
162 through direct $^{40}\text{Ar}/^{39}\text{Ar}$ dating of the tephtra or ^{14}C dating of adjacent organic material (Table 1).
163 When a radiometric or tephtra date was obtained on a unit of sediment, the depth of the mid-point of
164 this unit was used for the date in the age modelling. Both the age estimate and the associated errors
165 (standard deviation) are required for age-model construction. When the positive and negative
166 standard deviations were different, the larger value was used for age-model construction. In cases
167 where the error measurements on the radiometric dates were unknown (e.g. site F2-92-P29), no
168 attempt was made to construct a harmonized age model.

169 Measured ^{14}C ages were transformed to calendar ages, to account for the variations in the
170 atmospheric $^{14}\text{C}/^{12}\text{C}$ ratio through time. Radiocarbon ages from marine sequences were corrected
171 before calibration to account for the reservoir effect whereby dates have old ages because of the
172 delay in exchange rates between atmospheric CO_2 and ocean bicarbonate and the mixing of young
173 surface waters with upwelled old deep waters. We used the IntCal13 and Marine13 calibration
174 curves for terrestrial and marine ^{14}C dates, respectively [Reimer *et al.*, 2013], which are the
175 calibration curves approved by the radiocarbon community [Hajdas, 2014]. Although studies have
176 shown that the radiocarbon ages of tree rings from the Southern Hemisphere (SH) are ca 40 yr older
177 than Northern Hemisphere (NH) trees formed at the same time [Hogg *et al.*, 2013], this difference is
178 smaller than the laboratory errors on most of the ^{14}C dates and, since the Marine13 calibration curve
179 does not distinguish between SH and NH sites, we use the NH IntCal13 calibration curve for all the
180 records.

181 The Marine13 calibration curve includes a default 400 yr reservoir correction. We adjusted
182 this correction factor for all the twenty six marine records included in the database using the regional
183 marine reservoir age (ΔR) in the Marine Reservoir Correction Database
184 (<http://calib.qub.ac.uk/marine/>). For twenty marine records, the correction factor was based on a
185 maximum of the 20 closest sites within 1,000 km to a specific site; for the remaining 6 marine



186 records this factor was based on a maximum of the 20 closest sites within 3,000 km. When ΔR s were
187 homogeneous, a value ± 100 years, over this area we used the mean of the 10 sites within 100 km to
188 provide a reservoir correction for the site. When there was heterogeneity in ΔR values within the
189 3,000 km target area, we selected only the sites with homogeneous ΔR within 100-200 km. Temporal
190 variations of ΔR were not taken into account since they are currently not well established for many
191 locations.

192 For periods beyond the limit of ^{14}C dating (~ 45 ka) and for the few records without
193 radiometric dating, additional chronological control points were obtained based on “event
194 stratigraphy”, specifically the identification of D-O warming events and Marine Isotope Stage (MIS)
195 boundaries (Table 1). No assumption was made that core tops were modern for both marine and
196 terrestrial cores. The ages of D-O warming events and those of the MIS boundaries were based on
197 the stratigraphy of core MD95-2042, southern Iberian margin (Table 1). The similarity of the
198 planktonic foraminifera $\delta^{18}\text{O}$ record from MD95-2042 to the $\delta^{18}\text{O}$ record from Greenland allowed to
199 match ages of individual D-O cycles, while the benthic foraminifera $\delta^{18}\text{O}$ record from MD95-204
200 allowed to match ages of MIS boundaries [Shackleton *et al.*, 2000]. Both D-O and MIS ages were
201 directly transferred to the MD95-2042 pollen record. The chronology of this pollen record was in turn
202 transferred to the other European pollen records assuming synchronous afforestation during D-O
203 warming. The uncertainties for the event-based ages up to D-O 17 are from data summarized in
204 Wolff *et al.* [2010] and from AICC_2012 in NGRIP ice standard deviation [Bazin *et al.*, 2013] for older
205 events.

206 Non-radiocarbon dates are presented in the same BP notation as radiocarbon
207 determinations. The modern reference date is taken as 1950 AD, since this is the reference date for
208 the GICC05 chronology [Wolff *et al.*, 2010]).

209 Bayesian age modeling (e.g. using OxCAL, Bchron or BACON) requires information about
210 accumulation rates and other informative user-defined priors [Blaauw and Christen, 2011] that is
211 difficult to obtain for the relatively long ACER records. Moreover, BACON and Bchron [Haslett and



212 *Parnell, 2008, Parnell et al., 2008*] do not handle sudden shifts in accumulation rate very well, and
213 such shifts are not uncommon across deglaciation and stadial time periods. We therefore use the
214 classical age-modeling approach in the CLAM software [*Blaauw, 2010*], implemented in R (R version
215 3.3.1) [*R Development Core Team, 2016*], to construct the age model.

216 Several age models were built for each record using the calibrated distribution of the
217 radiometric dates: a) linear interpolation between dated levels; b) linear or higher order polynomial
218 regression; and c) cubic, smoothed or locally weighted splines (Table S2). Linear interpolation is
219 generally the most parsimonious solution for records with no age reversals. However, if any of the
220 regression or spline models provided a better fit to the calibrated age range of outliers from a linear
221 model, we selected the model that included most of the outliers. If none of the regression or spline
222 model provided a better fit, we used linear interpolation after excluding the outliers. The database
223 includes information on the single 'best' age-model and the 95% confidence interval estimated from
224 the 10,000 iterated age-depth models (weighted mean) for every sample depth.

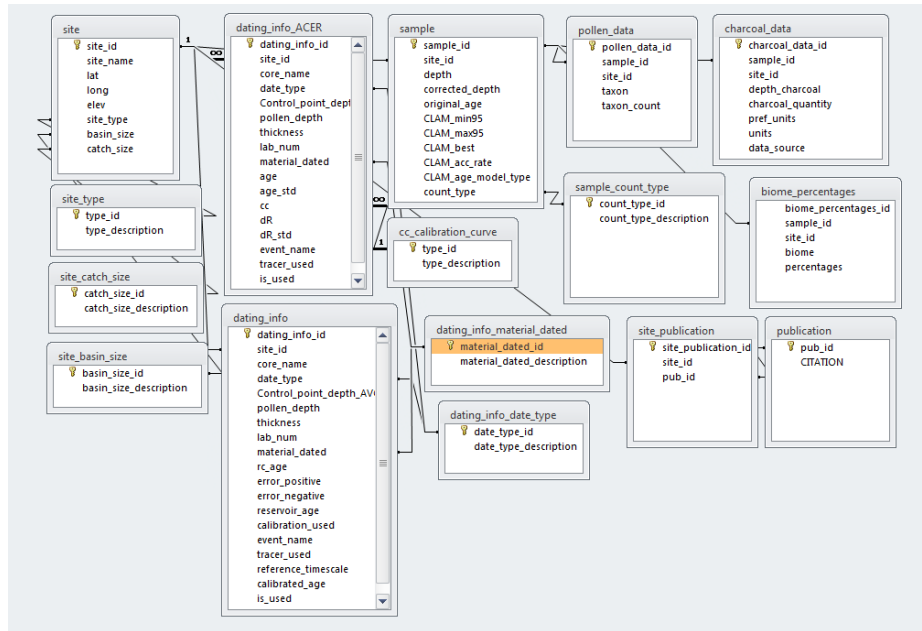
225

226 **2.3 The Structure of the Database**

227 The ACER pollen and charcoal data set is archived in a *Microsoft Access*TM relational database.

228 There are six main tables (Fig. 1).

229



230

231 *Figure 1 – ACER database structure in ACCESS format.*

232

233 (1) Site Metadata. This table includes the original site name, geographical coordinates (latitude
234 and longitude in decimal degrees, elevation in meters above or below sea level) and additional meta-
235 data including site type (marine or terrestrial), basin size, catchment size. Basin size and catchment
236 size determine the size of the area sampled by the record (or pollen source area: see Prentice, 1988),
237 but are not always recorded in the original publication or known very accurately. A categorical
238 classification (small, medium, large, very large) is recorded in the database where these categories
239 are specified by ranges in km². The details of the original publication of the data are also given in this
240 table.

241 (2) Sample data. The table records the identification number of each sample (sample id) at each
242 site (site id) and provides the depth of the sample (in cm from the surface). In only one site, core
243 MD04-2845, a corrected depth is provided on which the new age model is based. The pollen count
244 type (raw pollen count, pollen percentages given by the authors, or digitized percentage) is also
245 given. The original age of the sample according to the published age model when available and the



246 age determined from the best CLAM model (the min and the max at 95%, the accumulation rate and
247 the type of model used to obtain this age) are given.

248 (3) Pollen data. The pollen data are recorded as raw counts or as the pollen percentage of each
249 pollen and spore morphotype identified. The table records the identification number of each sample
250 (sample id), the taxon name and count/percentage. Although the taxon names were standardized
251 with respect to the use of terms such as type and to remove obvious spelling mistakes, no attempt
252 was made to ensure that the names are taxonomically correct.

253 (4) Charcoal data. The table records the identification number of each sample (sample id). The
254 charcoal data are recorded by depth (in cm from the surface), and information is given on the
255 quantity and unit of measurement, and data source. Charcoal abundance is quantified using a
256 number of different metrics, given for the majority in concentrations and for few of them in
257 percentages.

258 (5) Original dating information. This table contains information on dating for each core at each
259 site. The core name from the original publication is given, and the table provides information on date
260 type (conventional ^{14}C , AMS ^{14}C , $^{234}\text{U}/^{230}\text{Th}$, OSL, $^{40}\text{Ar}/^{39}\text{Ar}$, annual laminations, event stratigraphy,
261 TL), the average depth assigned to the data in the age-model construction, the dating sample
262 thickness, laboratory identification number, material dated (bulk, charcoal, foraminifera, pollen,
263 tephra, wood), measured radiometric age and associated errors. The marine reservoir age (and
264 associated error) and the radiocarbon calibration curve used in the construction of the original age
265 model, and the original calibrated age, are also given. Dates that are based on recognized events are
266 also listed, and identified by the name of the event (event name) and the type of record in which it is
267 detected (tracer used). The column "is_used" corresponds to the dates used by the authors for
268 building the original age models.

269 (6) ACER dating information. The ACER dating information table duplicates the original dating
270 information file, except that it provides information about the explicit corrections and the
271 harmonized control points used to produce the ACER age models (Table 1). Specifically, it gives the



272 calibration curve used (no calibration, INTCAL13, MARINE13), and the local reservoir age (and
 273 uncertainty) for marine cores.

274

275 *Table 1. Harmonized control points used for age models when radiometric ages (^{14}C , OSL, $^{40}\text{Ar}/^{39}\text{Ar}$,*

276 *$^{234}\text{U}/^{230}\text{Th}$) were not available.*

Event stratigraphy ^{1,2,3,4,5,6}		GICC05 ⁸ b1950	Tephra layers ⁸⁻¹⁹	ACER chronology Age $^{14}\text{C}^a$	ACER Age ka	Uncertainties ^{8,24} Years
		Age ka				
			K-Ah ⁹	6.28		130
			Mazama Ash ¹⁰	6.84		50
			Rotoma ¹¹	8.53		10
			U-Oki ¹²		10 ^b	300
Onset Holocene		11.65			11.65	50
			Rotorua ¹¹	13.08		50
MIS 1/2	D-O 1	14.6			14.6	93
			Rerewhakaaitu ¹³	14.7		95
			NYT ¹⁴		14.9 ^b	400
			Sakate ¹⁵	16.74		160
			Y-2 ¹⁶	18.88		230
LGM					21	
			Kawakawa/Oruanui ¹⁷	21.30		120
	D-O 2	23.29			23.29	298
MIS 2/3	D-O 3	27.73			27.73	416
			AT ⁹	24.83		90
	D-O 4	28.85			28.85	449
			TM-15		31 ^{b22}	8000
	D-O 5	32.45			32.45	566
	D-O 6	33.69			33.69	606
	D-O 7	35.43			35.43	661
			TM-18		37 ^{b22}	3000
	D-O 8	38.17			38.17	725
			Y-5 ¹⁶		39.28 ^b	110
			Akasuko ¹⁸	40.73		1096
	D-O 9	40.11			40.11	790
	D-O 10	41.41			41.41	817
	D-O 11	43.29			43.29	868
			Breccia zone ¹⁸	43.29		955
	D-O 12	46.81			46.81	956
	D-O 13	49.23			49.23	1015
	D-O 14	54.17			54.17	1150
			TM-19		55 ^{b22}	2000
	D-O 15	55.75			55.75	1196
	D-O 16	58.23			58.23	1256
MIS 3/4	D-O 17	59.39			59.39	1287



	onset HS 6	64.6 ⁶	64.6	1479
	D-O 18	65 ⁶	65	1518
MIS 4/5	D-O 19 (onset Ognon II)	72.28	72.28	1478
	D-O 20 (onset Ognon I)	76.4	76.4	1449
	C 20 (stadial I)	77 ⁶	77	1476
	MS-insolation 15°S*	81	81	1504
MIS 5.1	D-O 21 (onset St Germain II)	82.9 ⁵	82.9	1458
	C 21	85 ⁷	85	1448
		Vico ¹⁹	87 ^b	7000
		Aso-4 ²⁰	89 ^b	7000
		Ash-10 ²¹	100 ^b	1540
MIS 5/6			135 ²³	2500

277

278 *Middle of “high” magnetic susceptibility record zone (consistently <50 SI units) tied to low in insolation for
 279 January 15°S [Gosling *et al.*, 2008].

280 ^a Ages in ¹⁴C that were calibrated for the construction of the age model.

281 ^b Ages in ⁴⁰Ar/³⁹Ar or ⁴⁰K/⁴⁰Ar

282 K-Ah: Kikai-Akahoya; U-Oki: Ulleungdo-U4; NYT: Neapolitan Yellow Tuff ; AT: Aira Tephra; K-Tz: Kikai-
 283 Tozurahara

284 ¹[Shackleton *et al.*, 2000], ²[Shackleton *et al.*, 2004], ³[Svensson *et al.*, 2006], ⁴[Svensson *et al.*, 2008], ⁵[Sánchez
 285 Goñi, 2007], ⁶[Sanchez Goñi *et al.*, 2013], ⁷[McManus *et al.*, 1994], ⁸[Wolff *et al.*, 2010], ⁹[Smith *et al.*, 2013], ¹⁰
 286 [Grigg and Whitlock, 1998], ¹¹[Newnham *et al.*, 2003], ¹²[Smith *et al.*, 2011], ¹³[Shane *et al.*, 2003], ¹⁴[Deino *et al.*
 287 *et al.*, 2004], ¹⁵[Katoh *et al.*, 2007], ¹⁶[Margari *et al.*, 2009], ¹⁷[Vandergoes *et al.*, 2013], ¹⁸[Sawada *et al.*, 1992],
 288 ¹⁹[Magri and Sadori, 1999], ²⁰[Nakagawa *et al.*, 2012], ²¹[Whitlock *et al.*, 2000], ²²[Wulf *et al.*, 2004];

289 ²³[Henderson and Slowey, 2000], ²⁴[Bazin *et al.*, 2013] (italics: uncertainties of the closest age in AICC_2012 in
 290 NGRIP ice standard deviation).

291

292 Additional tables document the codes used in the main tables for e.g. basin type, basin size, date
 293 type, material dated, calibration curve and biome percentage table that includes selected biomes
 294 provided by the authors (Table 1). The taxa defining the pollen percentages of the main forest
 295 biomes are those originally published by the authors in the Quaternary Science Reviews special issue
 296 [Fletcher *et al.*, 2010; Hessler *et al.*, 2010; Jimenez-Moreno *et al.*, 2010; Takahara *et al.*, 2010]. The
 297 taxa defining the pollen percentages of the main biomes from Africa (Mfabeni, Rumuiku) Australia
 298 (Caledonia Fen, Wangoom) and New Zealand (Kohuora) not included in this issue are described in the
 299 supplementary information.



300 Each table of the ACCESS database is also available as .csv file: a) Site, b) Sample (original depth-
 301 age model and ACER depth-age model), c) Dating info (original dating information), d) dating info
 302 ACER (harmonized dating information from this work), e) pollen data (raw data or digitized pollen
 303 percentages; pollen percentages of different biomes) (Table 2), f) unique taxa in database (list of all
 304 the identified taxa), g) charcoal data (raw or digitized).

305

306 *Table 2 – Biomes for which the pollen percentages data are included in the ACER database. Bo forest:*
 307 *Boreal forest; Te mountain forest: Temperate mountain forest; Te forest: Temperate forest; WTe*
 308 *forest: Warm-Temperate forest; Tr forest: Tropical forest; Subtr forest: Subtropical forest; SE Pine*
 309 *forest: Southeastern Pine forest; Gr: Grasslands; Sav: Savanah. In Europe, Te forest includes*
 310 *Mediterranean and Atlantic forests.*

311

Europe	North	Tropics		East Asia	New Zealand	Australia
	America	American	African			
	Bo forest	Te mountain forest		Bo forest		
Te forest	Te forest	WTe forest		Te forest	Te forest	WTe forest
	WTe forest	Tr forest		WTe forest	WTe forest	Te mountain forest
	SE Pine Forest	Gr		Subtr forest		Sav
				Gr		

312

313

314 **3 Results**

315 **3.1 The ACER pollen and charcoal database**

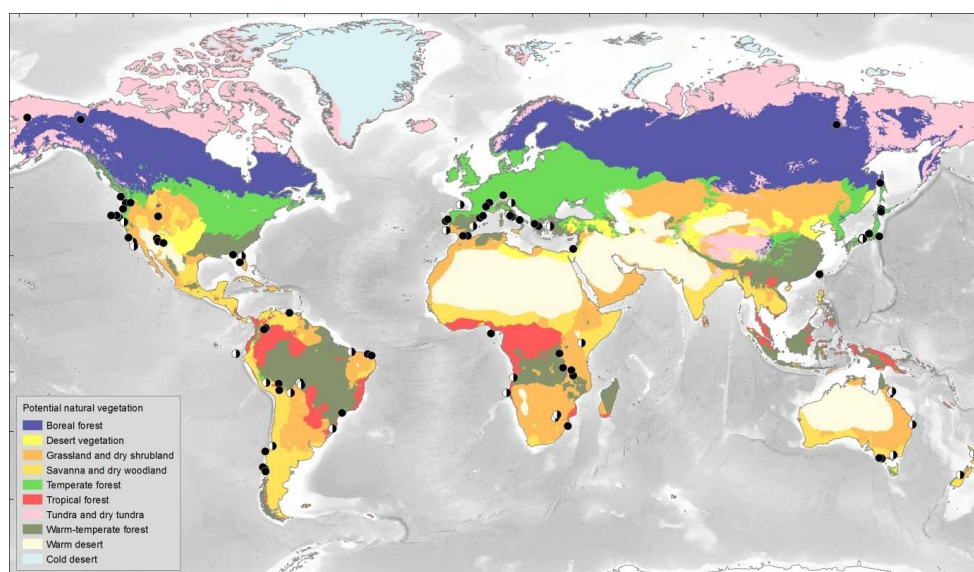
316 ACER database comprises all available pollen and charcoal records covering all or part of the
 317 last glacial (73 to 15 ka) as of July 2015. It contains 93 well-resolved pollen records (< 1,000 years



318 between samples), 32 of which include charcoal data, from all the major potential present-day
319 biomes (Fig. 2). There are 2486 unique pollen and spore taxa in the database.

320 Harmonized age models were constructed for 86 out of the 93 records (Table S2 in the
321 supplementary information). The seven sites without harmonized age models are: F2-92-P29 (no
322 radiocarbon age errors available); Bear Lake (pollen was counted on one core but sample depths
323 could not be correlated with the cores used for dating); EW-9504 and ODP 1234 (original age models
324 based on correlation with another core, but tie point information was not available); Okarito Pakihi
325 (no dating information available) and Wonderkrater borehole 3 (multiple age reversals). The well-
326 known site of La Grande Pile [*de Beaulieu and Reille, 1992*] is not included in the ACER database
327 because the high-resolution data are not publicly available. Other sequences, such as Sokli in Finland,
328 were fragmented and could not be used (Table S1). These sites are shown at the bottom of the
329 supplementary Table S1.

330



331

332 **Figure 2** - Map with location of the 93 marine and terrestrial sites (pollen: black circles, charcoal:
333 white circles) having resolution higher than 1 sample per 1000 years covering part or all the last
334 glacial (MIS 4, 3 and 2). Present-day potential natural vegetation after [*Levvasseur et al., 2012*].
335



336

337 **3.2 Harmonized *versus* original age models**

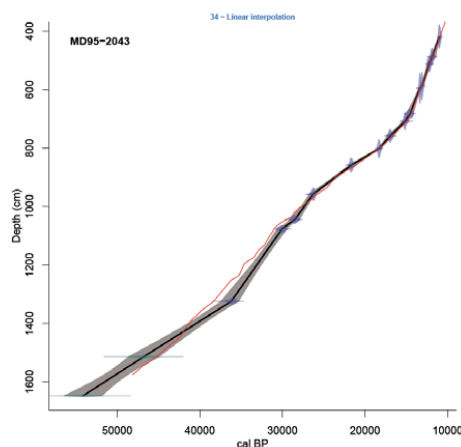
338 We generated a total of 774 different age models. The age models of 45 records are based on
339 linear interpolation (Table S2 in the supplementary information). The age models of the other
340 records are derived from smooth or locally weighted splines (e.g. Lake Caço, Brazil; Fargher Lake,
341 North America; ODP1078C, southeastern Atlantic margin) or polynomial regression (e.g. Hanging
342 Lake and Carp Lake, North America; Lake Fuquene, Colombia; Valle di Castiglione, Europe) to include
343 as many as possible of the available radiometric dates. Since the focus for age modeling was the last
344 glacial period, age models for the Holocene (11.65ka - present) and Last Interglacial *sensu lato*
345 intervals (135ka -72.28 ka) are not necessarily well constrained.

346 Selected examples of the original and harmonized age models are illustrated in Figures 3 and
347 4. The original age model of marine core MD95-2043, western Mediterranean Sea (Figure 3a, red
348 curve) was based on tuning the mid-points of the cold to warm D-O transitions with the equivalent
349 mid-points in the alkenone-based sea-surface temperature (SST) record [Cacho *et al.*, 1999]. The
350 harmonized age model (black) is based on 21 ¹⁴C ages and two isotopic stratigraphic events (D-O 12
351 and D-O 14). The two age models are similar, with a mismatch of less than 1,000 years for periods
352 older than 35 ka and narrow uncertainties (Fig. 3a). In contrast, the original age model of the
353 terrestrial sequence of Valle di Castiglione, central Italy, published in Fletcher *et al.* (2010) differs
354 substantially, by several millennia, from the harmonized model in the interval between 50 and 30 ka
355 and has large uncertainties (Fig. 3b). This age model was based on two calibrated ¹⁴C dates, one
356 ⁴⁰Ar/³⁹Ar tephra age (Neapolitan Yellow Tuff, Table 2) and the identification of D-O 8, 12 and 14 while
357 the new age model takes into account the entire number of ¹⁴C dates (eight), one ⁴⁰Ar/³⁹Ar tephra
358 age and one GICC05-event stratigraphic age (identification of D-O 21). It derives from a 3rd order
359 polynomial regression model to take into account as many as possible of the radiometric ages
360 available (Table S2 in the supplementary information).

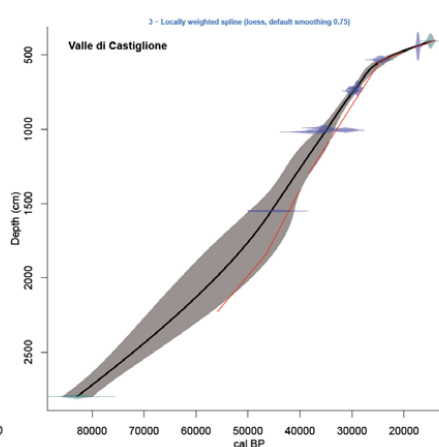


361

362 a.



b.



363

364 Figure 3- a) Linear age model of the marine core MD95-2043, and b) 3rd order polynomial age model
365 of the terrestrial sequence Valle di Castiglione. Red line: original age model with the control points,
366 Black line: harmonized age model based on radiometric dating and event stratigraphy. Blue:
367 calibrated ¹⁴C distribution. Green: non-¹⁴C age distribution (⁴⁰Ar/³⁹Ar, ²³⁴U/²³⁰Th, OSL, event
368 stratigraphy). Grey shadow: age uncertainties.

369

370 The original age model for marine core ODP 1233 C from the southern Pacific Ocean off
371 southern Chile was based on 19 AMS ¹⁴C dates calibrated using Calpal 2004 [Heusser *et al.*, 2006] and
372 is very similar to the harmonized age model (Figure 4a). The use of the new INTCAL13 calibration
373 curve is sufficient to explain the small differences between the original and harmonized age models.
374 In contrast, there are major differences between the original and harmonized age models for the
375 terrestrial pollen record of Toushe, Taiwan (Figure 4b). The original age model [Liew *et al.*, 2006] was
376 based on 24 uncalibrated radiometric dates for the 0-24 ka interval, and two dated isotopic events,
377 MIS 3/4 and MIS 4/5, which were dated following Martinson *et al.* [1987] to 58.96 ka and 73.91 ka
378 respectively. The harmonized age model is based on calibrated ages from 3 AMS ¹⁴C and 28



379 conventional ^{14}C dates and dating of the MIS 3/4 and MIS 4/5 boundaries. In the ACER chronology,
380 these two events are dated to 59.39 ka and 72.28, respectively. In combination, these differences
381 produce substantially younger ages (by up to 5,000 years) for the interval between 50-26 ka than in
382 the original age model.

383

384

385

386

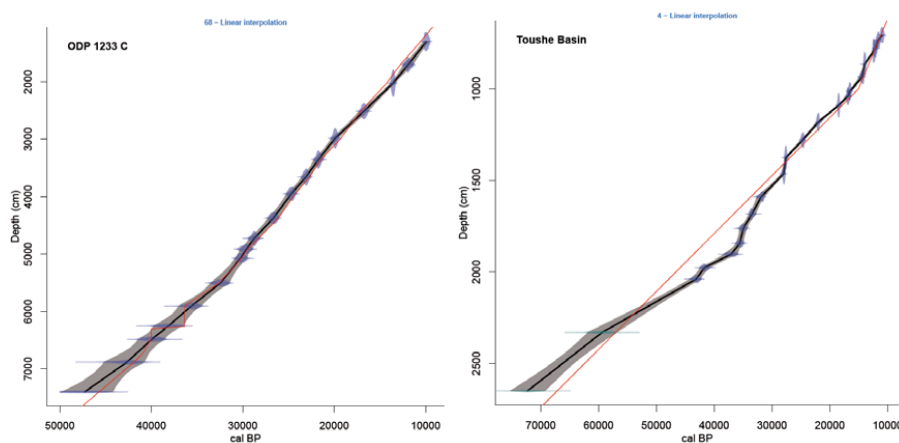
387

388

389

390 a.

b.



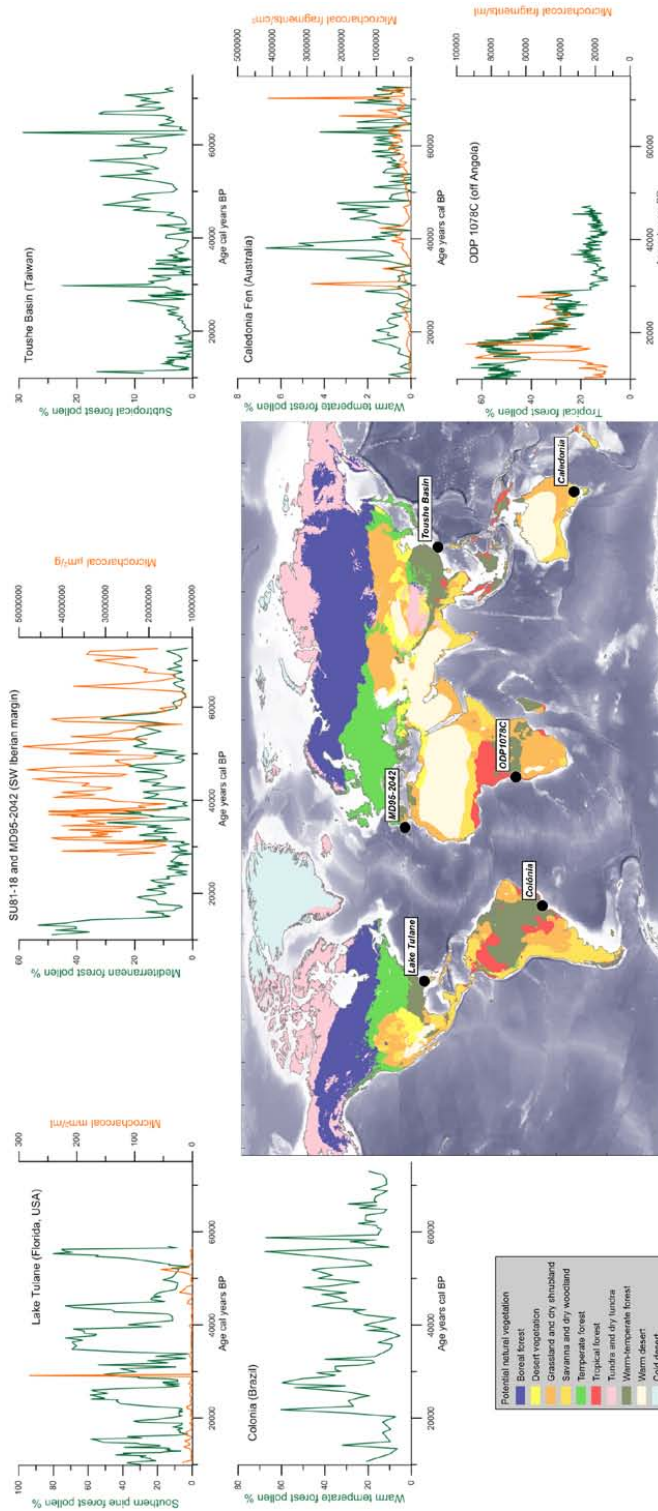
391

392 Figure 4- a) Linear age model of the marine core ODP 1233 C, and b) Linear age model of the
393 terrestrial sequence Toushe (Taiwan). Red line: original age model with the control points, Black line:
394 harmonized age model based on radiometric dating. Blue: calibrated ^{14}C distribution. Green: non- ^{14}C
395 age distribution ($^{40}\text{Ar}/^{39}\text{Ar}$, $^{234}\text{U}/^{230}\text{Th}$, OSL, event stratigraphy). Grey shadow: age uncertainties.

396



397 Figure 5 additionally illustrates pollen and microcharcoal data plotted against the harmonized age
398 models for few sites from different biomes. This figure highlights the regional response of the
399 vegetation and fire regime to the D-O events.





401 *Figure 5 – Pollen (black) and charcoal (orange) curves from six sites plotted against the harmonized*
402 *age model.*

403 **3.3 Vegetation and climate response to the contrasting D-O 8 and D-O 19 warming events.**

404 Comparison of the vegetation and climate response to warming events in two different
405 regions provides an example of the importance of developing harmonized chronologies. D-O 19 and
406 D-O 8 are iconic D-O events, characterized by strong warming in Greenland followed by long
407 temperate interstadials of 1,600 (GI 19) and 2,000 (GI 8) years respectively [Wolff *et al.*, 2010]. D-O 8
408 occurred ca 38.17 ka b1950 AD and was marked by an initial short-lived warming of ca 11°C, whereas
409 D-O 19 (ca 72.28 ka b1950 AD) was characterised by a maximum warming of ca 16°C. The difference
410 in the magnitude of warming suggests that the Northern Hemisphere monsoons would be stronger
411 during D-O 19 than D-O 8, but this is not consistent with speleothem evidence from Hulu Cave
412 (China) indicating that monsoon expansion was more marked during D-O 8 than during D-O 19
413 [Wang *et al.*, 2001] (Fig. 6). Sanchez Goñi *et al.* [2008] argued that the smaller increase in CH₄ during
414 D-O 19, by ca 100 ppbv, than during D-O 8, by ca 200 ppbv, was because the expansion of the East
415 Asian monsoon (and hence of regional wetlands) was weaker during D-O 19 due to the differences in
416 precession during the two events (Fig. 6). Differences in the strength of the monsoons between GI 8
417 (precession minima, high seasonality) and GI 19 (precession maxima, low seasonality) can also be
418 tested using evidence from the pollen record of Toushe Basin, which lies under the influence of the
419 East Asian monsoon. This record shows a similar development of moisture-demanding subtropical
420 forest, during the two interstadials (Fig. 6), and thus does not support the argument that the East
421 Asian monsoon was weaker/less expanded during GI 19 than during GI 8. However, Toushe Basin lies
422 in the tropical belt (23°N) and is likely to be less sensitive to changes in monsoon extent than more
423 marginal sites such as Hulu Cave (32°N).

424 Previous works have also hypothesized that the Mediterranean forest and climate were
425 tightly linked to the Asian and African monsoon through the Rodwell and Hoskins zonal mechanism



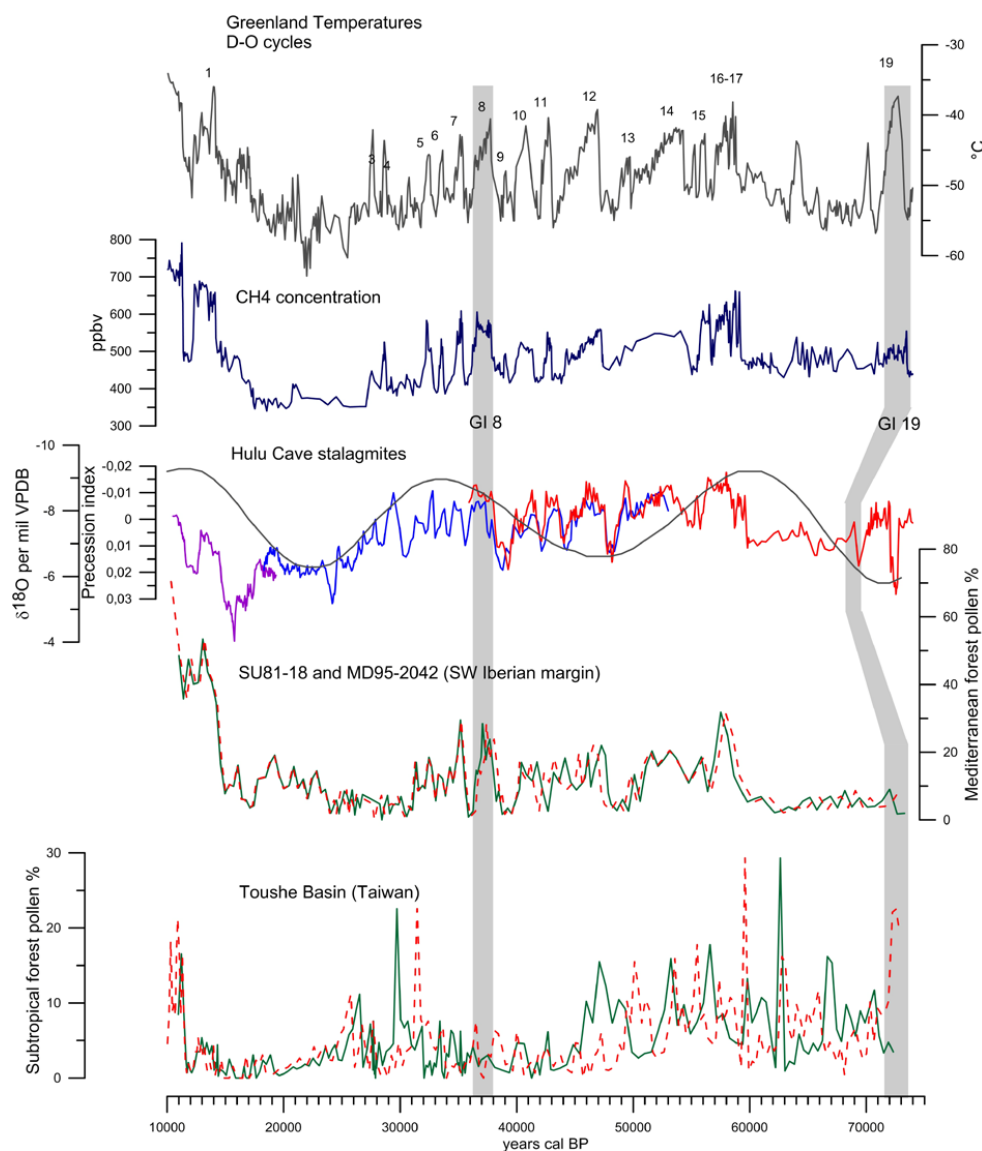
426 [Marzin and Braconnot, 2009; Sanchez Goñi et al., 2008] or through shifts in the mean latitudinal
427 position of the ITCZ [Tzedakis et al., 2009]. Data from Hulu cave [Wang et al., 2001] and the western
428 Mediterranean region (MD95-2042 and SU81-18 twin pollen sequences) show that during warming
429 events occurring at minima in precession, such as D-O 8, monsoon intensification is stronger and
430 associated with a marked seasonality in the Mediterranean region (strong summer dryness) and,
431 therefore, a strong expansion of the Mediterranean forest and decrease in the summer dry-
432 intolerant Ericaceae (Fig. 6) [Sánchez Goñi et al., 1999; Sánchez Goñi et al., 2000]. Actually, we
433 observe parallel strong and weak increases in East Asian monsoon and Mediterranean forest during
434 GI 8 and GI 19, respectively. However, here again there is a discrepancy between the harmonized
435 Toushe pollen sequence and that from the Hulu cave and the western Mediterranean region: the
436 Mediterranean forest and monsoon during D-O 8 strongly increased while the subtropical forest
437 cover weakly expanded. The different latitudinal position of the Toushe Basin (23°N) in tropical
438 region and that of the Hulu Cave (32°N) and the southern Iberian margin sequence (37°N) both in the
439 subtropical region could explain such a discrepancy. A comprehensive analysis of differences in the
440 magnitude of monsoon expansion between D-O 8 and D-O 19 is now possible because of the creation
441 of robust and standardised age models for the ACER records.

442

443

444

445



446

447 Figure 6 - Comparison of pollen sequences from the Toushe Basin (Taiwan) and the SW Iberian margin
448 (cores MD95-2042 [Desprat et al., 2015; Sanchez Goñi et al., 2008] and SU 81-18 (23500-10000 cal
449 years BP) [Lézine and Denèfle, 1997]) for the interval 73-23.5 ka. Green line: new harmonized age
450 model, red dashed line: original age model. Grey vertical bands indicate the duration of GI 8, GI 16-17
451 and GI 19. Also shown the comparison with the Greenland temperature record (black) [Huber et al.,
452 2006; Landais et al., 2005; Sanchez Goñi et al., 2008], atmospheric CH₄ concentration (blue) record



453 *[Chappellaz et al., 1997; Flückiger et al., 2004], compiled Hulu Cave $\delta^{18}\text{O}$ speleothem records (PD in*
454 *purple, MSD in green, and MSL in blue) [Wang et al., 2001], and precession index [Laskar et al.,*
455 *2004]. Note the mismatch in the timing of GI 19 between the Greenland and pollen harmonized age*
456 *models and the chronology of Hulu Cave.*

457 **4. Conclusions**

458 The ACER pollen and charcoal database (ACER 1.0) comprises all available pollen and charcoal
459 records covering part or all of the last glacial, as of July 2015. We foresee future updates of the ACER
460 database by the research community with newly published pollen and charcoal records. For
461 consistency age models for new sites should be constructed using the strategy described here.

462 The harmonization of the ACER age models in the ACER 1.0 database increases the
463 consistency between records by (a) calibrating all the radiocarbon dates using the recommended
464 INTCAL13 and MARINE13 calibration curves, (b) using the same ages for non-radiometric control
465 points and basing these on the most recent Greenland ice core chronology (GICC05), and (c) using
466 the CLAM software to build the age models and taking account of dating uncertainties. While these
467 harmonized age models may not be better than the original models, they have the great advantage
468 of ensuring comparability between pollen and charcoal records from different regions of the world.
469 As we have shown in the preliminary analyses of monsoon-related vegetation changes during D-O 8
470 and D-O 19, this will facilitate regional comparisons of the response to rapid climate changes.

471 The same strategy for age-model harmonization is now being applied to the sea-surface
472 temperature records from the last glacial that have been compiled by the ACER-INTIMATE group
473 (<http://www.ephe-paleoclimat.com/acer/ACER%20INTIMATE.htm>). This will ensure that the
474 terrestrial and marine databases share a common chronological framework, a considerable step
475 towards improving our knowledge of the interactions between oceans and land that underlie the
476 nature and timing of abrupt climatic changes.



477

478 **Data availability**

479 Supplementary data are available at <https://doi.org/10.1594/PANGAEA.870867>

480 **Author contributions.** MFSG, SD and ALD, developed the harmonized age models, ALD developed the
481 ACER database in ACCESS, FB participated in the construction of age models, JMPM extracted the
482 pollen percentage of the dominant biomes from the European sequences compiled in the ACER
483 database. MFSG and SPH write the manuscript. The remaining authors are listed alphabetically and
484 are data contributors (see their respective dataset on Table S1 in the Supplement link). All data
485 contributors (listed on Table S1) were contacted for authorisation of data publishing and offered co-
486 authorship. All the authors have critically reviewed the manuscript. Any use of trade, firm, or product
487 names is for descriptive purposes only and does not imply endorsement by the U.S. Government.

488

489

490 **Acknowledgements**

491 We wish to thank the QUEST-DESIRE (UK-France) bilateral project, the INQUA International Focus
492 Group ACER and the INTIMATE-COST action for funding a suite of workshops to compile the ACER
493 pollen and charcoal database and the workshop on ACER Chronology that allow setting the basis for
494 harmonizing the chronologies. We thank Maarten Blaauw for constructive discussions leading to the
495 construction of age models. JMPM was funded by a Basque Government post-doctoral fellowship
496 (POS_2015_1_0006) and SPH by the ERC Advanced Grant GC2.0 : Unlocking the past for a clearer
497 future. We thank V. Hanquiez for drawing Figure 2.

498

499



500 **Figures & Tables**

501 Figure 1 – ACER database structure in ACCESS format.

502

503 Figure 2 – Map with location of the 93 marine and terrestrial pollen sites covering part or all the last
504 glacial (MIS 4, 3 and 2). Sites have better resolution than 1 sample per 1000 years. Present-day
505 potential natural vegetation after [Levvasseur *et al.*, 2012].

506

507 Figure 3 –a) Linear age model of the marine core MD95-2043, and b) 3rd order polynomial age model
508 of the terrestrial sequence Valle di Castiglione (Italy). Red line: original age model with the control
509 points, Black line: harmonized age model with based on radiometric dating and event stratigraphy.
510 Blue: calibrated ¹⁴C distribution. Green: non-¹⁴C age distribution (Ar/Ar, OSL, event stratigraphy).
511 Grey shadow: age uncertainties.

512

513 Figure 4- a) Linear age model of the marine core ODP 1233 C, and b) Linear age model of the
514 terrestrial sequence Toushe (Taiwan). Red line: original age model with the control points, Black line:
515 harmonized age model with based on radiometric dating and event stratigraphy. Blue: calibrated ¹⁴C
516 distribution. Green: non-¹⁴C age distribution (Ar/Ar, OSL, event stratigraphy). Grey shadow: age
517 uncertainties.

518

519 Figure 5 – Pollen (black) and charcoal (orange) curves from six sites plotted against the harmonized
520 age model.

521

522 Figure 6 - Comparison of pollen sequences from the Toushe Basin (Taiwan) and the SW Iberian
523 margin (cores MD95-2042 [Desprat *et al.*, 2015; Sanchez Goñi *et al.*, 2008] and SU 81-18 (23500-
524 10000 cal years BP [Lézine and Denèfle, 1997]) for the interval 73-23.5 ka . Green line: new
525 harmonized age model, red dashed line: original age model. Grey vertical bands indicate the duration



526 of GI 8, GI 16-17 and GI 19. Also shown the comparison with the Greenland temperature record
527 (black) [Huber *et al.*, 2006; Landais *et al.*, 2005; Sanchez Goñi *et al.*, 2008], atmospheric CH₄
528 concentration (blue) record [Chappellaz *et al.*, 1997; Flückiger *et al.*, 2004], compiled Hulu Cave δ¹⁸O
529 speleothem records (PD in purple, MSD in green, and MSL in blue) [Wang *et al.*, 2001], and
530 precession index [Laskar *et al.*, 2004]. Note the mismatch in the timing of GI 19 between the
531 Greenland and pollen harmonized age models and the chronology of Hulu Cave.

532

533 Table 1. Harmonized control points used for age models when radiometric ages (¹⁴C, OSL, ⁴⁰Ar/³⁹Ar,
534 ²³⁴U/²³⁰Th) were not available.

535

536 Table 2 – Biomes for which the pollen percentages data are included in the ACER database. Bo forest:
537 Boreal forest; Te mountain forest: Temperate mountain forest; Te forest: Temperate forest; WTe
538 forest: Warm-Temperate forest; Tr forest: Tropical forest; Subtr forest: Subtropical forest; SE Pine
539 forest: Southeastern Pine forest; Gr: Grasslands and dry shrublands; Sav: Savanah. In Europe, Te
540 forest refers to Mediterranean and Atlantic forests.

541

542

543



544 **References:**

- 545 Andersen, K. K., Svensson, A., Johnsen, S.J., Rasmussen, S.O., Bigler, M., Röthlisberger, R., Tuth, U.,
546 Siggaard-Andersen, M.-L., Steffensen, J.P., Dahl-Jensen, D., Vinther, B. M., Clausen, H.B., The
547 Greenland Ice Core Chronology 2005, 15-42 ka. Part 1: constructing the time scale, *Quaternary Sci.*
548 *Rev.*, 25, 3246-3257 (2006).
- 549 Bazin, L., Landais, A., Lemieux-Dudon, B., Toyé Mahamadou Kele, H., Veres, D., Parrenin, F.,
550 Martinerie, P., Ritz, C., Capron, E., Lipenkov, V., Loutre, M. F., Raynaud, D., Vinther, B., Svensson, A.,
551 Rasmussen, S. O., Severi, M., Blunier, T., Leuenberger, M., Fischer, H., Masson-Delmotte, V.,
552 Chappellaz, J., Wolff, E., An optimized multi-proxy, multi-site Antarctic ice and gas orbital chronology
553 (AICC2012): 120-800 ka, *Clim. Past*, 9, 1715-1731 (2013).
- 554 Blaauw, M., Methods and code for 'classical' age-modelling of radiocarbon sequences, *Quatern.*
555 *Geochrono.*, 5, 512-518 (2010).
- 556 Blaauw, M., and Christen, J. A., Flexible paleoclimate age-depth models using an autoregressive
557 gamma process. *International Society for Bayesian Analysis*, 3, 457-474 (2011).
- 558 Bond, G., and Lotti, R., Icebergs discharges into the North Atlantic on millennial time scales during the
559 Last Glaciation, *Science*, 267, 1005-1009, (1995).
- 560 Bonnefille, R., and Chalié F., Pollen-inferred precipitation time-series from equatorial mountains,
561 Africa, the last 40 kyr BP, *Global Planet. Change*, 26, 25-50, (2000).
- 562 Bronk Ramsey, C., Development of the radiocarbon calibration program OxCal, *Radiocarbon*, 43, 355-
563 363, (2001).
- 564 Burrows, M. T., Schoeman, D. S., Buckley, L. B., Moore, P.J., Poloczanska, E. S., Brander, K. M., Brown,
565 C., Bruno, J. F., Duarte, C. M., Halpern, B. S., Holding, J., Kappel, C. V., Kiessling, W., O'Connor, M. I.,
566 Pandolfi, J. M., Parmesan, C., Schwing, F. B., Sydeman, W. J., Richardson, A. J., The Pace of Shifting
567 Climate in Marine and Terrestrial Ecosystems, *Science*, 334, 652-655, (2011).
- 568 Burrows, M. T., Schoeman, D. S., Richardson, A. J., Garcia Molinos, J., Hoffmann, A., Buckley, L. B.,
569 Moore, P. J., Brown, C. J., Bruno, J. F., Duarte, C. M., Halpern, B. S., Hoegh-Guldberg, O., Kappel, C. V.,
570 Kiessling, W., O'Connor, M. I., Pandolfi, J. M., Parmesan, C., Sydeman, W. J., Ferrier, S., Williams, K.
571 J. Poloczanska, E. S., Geographical limits to species-range shifts are suggested by climate velocity,
572 *Nature*, 507, 492-495, (2014).
- 573 Cacho, I., J. O. Grimalt, C. Pelejero, M. Canals, F. J. Sierro, J. A. Flores, and Shackleton, N. J.,
574 Dansgaard-Oeschger and Heinrich event imprints in Alboran Sea paleotemperatures,
575 *Paleoceanography*, 14, 698-705 (1999).
- 576 Capron, E., Landais, A., Chappellaz, J., Schilt, A., Buiron, D., Dahl-Jensen, D., Johnsen, S. J., Jouzel, J.,
577 Lemieux-Dudon, B., Loulergue, L., Leuenberger, M., Masson-Delmotte, V., Meyer, H., Oerter, H.,
578 Stenni, B., Millennial and sub-millennial scale climatic variations recorded in polar ice cores over the
579 last glacial period, *Clim. Past*, 6, 345-365 (2010).



- 580 Chappellaz, J., T. Blunier, S. Kints, A. Dällenbach, J.-M. Barnola, J. Schwander, D. Raynaud, and
581 Stauffer, B., Changes in the atmospheric CH₄ gradient between Greenland and Antarctica during the
582 Holocene, *Journal of Geophysical Research*, 102, 987-915,997 (1997).
- 583 Dansgaard, W., S. Johnsen, H. B. Clausen, D. Dahl-Jensen, N. Gundestrup, C. U. Hammer, and
584 Oeschger, H., North Atlantic climatic oscillations revealed by deep Greenland ice cores, in *Climate
585 processes and climate sensitivity*, edited by J. E. Hansen and T. Takahashi, pp. 288 - 298, American
586 Geophysical Union, Washington, (1984).
- 587 de Beaulieu, J.-L., and Reille, M., The last climatic cycle at La Grande Pile (Vosges, France). A new
588 pollen profile, *Quaternary Sci. Rev.*, 11, 431-438 (1992).
- 589 de Beaulieu, J. L., and Reille, M., A long Upper Pleistocene pollen record from Les Echets, near Lyon,
590 France, *Boreas*, 13, 111-132 (1984).
- 591 Deino, A. L., Orsi, G., de Vita, S. and Piochi, M. The age of the Neapolitan Yellow Tuff caldera-forming
592 eruption (Campi Flegrei caldera – Italy) assessed by 40Ar/39Ar dating method, *Journal Volcanol.
593 Geoth. Res.*, 133, 157-170 (2004).
- 594 Desprat, S., P. M. Diaz Fernandez, T. Coulon, L. Ezzat, J. Pessarossi-Langlois, L. Gil, C. Morales-Molino,
595 and Sanchez Goñi, M. F., *Pinus nigra* (European black pine) as the dominant species of the last glacial
596 pinewoods in south-western to central Iberia: a morphological study of modern and fossil pollen, *J.
597 Biogeogr.*, 42, 1998-2009 (2015).
- 598 Eshel, G., Mediterranean climates, *Israel J. Earth Sci.*, 51, 157-168 (2002).
- 599 Fletcher, W. J., et al. (2010), Millennial-scale variability during the last glacial in vegetation records
600 from Europe, *Quaternary Sci. Rev.*, 29, 2839-2864.
- 601 Flückiger, J., T. Blunier, B. Stauffer, J. Chappellaz, R. Spahni, K. Kawamura, J. Schwander, T. F. Stocker,
602 and Dahl-Jensen, D., N₂O and CH₄ variations during the last glacial epoch: insight into global
603 processes, *Global Biogeochem. Cy.*, 18, doi: 10.1029/2003GB002122, (2004).
- 604 Gosling, W. D., Bush, M. B., Hanselman, J. A. and Chepstow-Lusty, A., Glacial-interglacial changes in
605 moisture balance and the impact on vegetation in the southern hemisphere tropical Andes
606 (Bolivia/Peru), *Palaeogeogr., Palaeocl.*, 259, 35-50, (2008).
- 607 Grigg, L. D., and Whitlock, C., Late-Glacial Vegetation and Climate Change in Western Oregon,
608 *Quaternary Research*, 49, 287-298 (1998).
- 609 Hajdas, I., Radiocarbon: calibration to absolute time scale, in *Treatise on Geochemistry*, edited by K.
610 Turekian and H. Holland, pp. 37-43, Elsevier, Oxford, (2014).
- 611 Harrison, S., and Sánchez Goñi, M. F., Global patterns of vegetation response to millennial-scale
612 variability and rapid climate change during the last glacial period, *Quaternary Sci. Rev.*, 29, 2957-2980
613 (2010).
- 614 Haslett, J., and Parnell, A. C., A simple monotone process with application to radiocarbon dated
615 depth chronologies, *J. Roy. Stat. Soc. C-APP*, 57, 399-418 (2008).



- 616 Heinrich, H., Origin and consequences of cyclic ice rafting in the northeast Atlantic ocean during the
617 past 130,000 years, *Quaternary Res.*, 29, 142-152 (1988).
- 618 Henderson, G. M., and Slowey, N. C., Evidence from U-Th dating against Northern Hemisphere
619 forcing of the penultimate deglaciation, *Nature*, 404, 61-66 (2000).
- 620 Hessler, I., L. Dupont, R. Bonnefille, H. Behling, C. González, K. F. Helmens, H. Hooghiemstra, J.
621 Lebamba, M.-P. Ledru, and Lézine, A.-M., Millennial-scale changes in vegetation records from tropical
622 Africa and South America during the last glacial, *Quaternary Sci. Rev.*, 29, 2882-2899 (2010).
- 623 Heusser, C. J., Palynology and phytogeographical significance of a Late-Pleistocene refugium near
624 Kalaloch, Washington, *Quaternary Res.*, 2, 189-201 (1972).
- 625 Heusser, C. J., Ice age vegetation and climate of subtropical Chile, *Palaeogeogr., Palaeoclimatol.,* 80, 107-
626 127 (1990).
- 627 Heusser, L. E., Heusser, C. J. and Piasias, N. Vegetation and climate dynamics of southern Chile during
628 the past 50,000 years: results of ODP Site 1233 pollen analysis, *Quaternary Sci. Rev.*, 25, 474-485
629 (2006).
- 630 Hogg, A. G., Hua, Q., Blackwell, P.G., Niu, M., Buck, C.E., Guilderson, T.P., Heaton, T.J., Palmer, J.G.,
631 Reimer, P.J., Reimer, R.W., Turney, C.S.M., Zimmerman, S.R.H., SHCAL13 Southern Hemisphere
632 calibration, 0-50,000 years cal BP, *Radiocarbon*, 55, 1889-1903 (2013).
- 633 Huber, C., M. Leuenberger, R. Spahni, J. Flückiger, J. Schwander, T. F. Stocker, S. Johnsen, A. Landais,
634 and Jouzel, J., Isotope calibrated Greenland temperature record over Marine Isotope Stage 3 and its
635 relation to CH₄, *Earth Planet. Sc. Lett.*, 243, 504-519 (2006).
- 636 Jimenez-Moreno, G., R. S. Anderson, S. Desprat, L. D. Grigg, E. C. Grimm, L. E. Heusser, B. F. Jacobs, C.
637 López-Martínez, C. L. Whitlock, and Willard, D. A., Millennial-scale variability during the last glacial in
638 vegetation records from North America, *Quaternary Sci. Rev.*, 29, 2865-2881(2010).
- 639 Johnsen, S. J., H. B. Clausen, W. Dansgaard, K. Fuhrer, N. Gundestrup, C. U. Hammer, P. Iversen, J.
640 Jouzel, B. Stauffer, and Steffensen, J. P., Irregular glacial interstadials in a new Greenland ice core,
641 *Nature*, 359, 311-313 (1992).
- 642 Katoh, S., K. Handa, M. Hyodo, H. Sato, T. Nakamura, T. Yamashita, and Danhara, T., Estimation of
643 eruptive ages of the late Pleistocene tephra layers derived from Daisen and Sambe Volcanoes
644 based on AMS-¹⁴C dating of the moor sediments at Ohnuma Moor in the Chugoku
645 Mountains, Western Japan, *Nature and Human Activities*, 11, 29-50 (2007).
- 646 Landais, A., V. Masson-Delmotte, J. Jouzel, D. Raynaud, S. Johnsen, C. Huber, M. Leuenberger, J.
647 Schwander, and Minster, B., The glacial inception as recorded in the NorthGRIP Greenland ice core:
648 timing, structure and associated abrupt temperature changes, *Clim. Dyn.*, DOI 10.1007/s00382-005-
649 0063-y (2005).
- 650 Laskar, J., P. Robutel, F. Joutel, M. G. Tineau, A. C. M. Correia, and Levrard, B., A long-term numerical
651 solution for the insolation quantities of the Earth, *A&A*, 428(1), 261-285 (2004).



- 652 Levvasseur, G., M. Vrac, D. M. Roche, and Paillard, D., Statistical modelling of a new global potential
653 vegetation distribution, *Environmental Research Letters*, 7, 044019 (2012).
- 654 Lézine, A.-M., and Denèfle, M., Enhanced anticyclonic circulation in the eastern North Atlantic during
655 cold intervals of the last deglaciation inferred from deep-sea pollen records, *Geology*, 25, 119-122
656 (1997).
- 657 Liew, P.-M., S.-Y. Huang, and Kuo, C.-M., Pollen stratigraphy, vegetation and environment of the last
658 glacial and Holocene—A record from Toushe Basin, central Taiwan, *Quatern. Int.*, 147, 16-33 (2006).
- 659 Loarie, S. R., P. B. Duffy, H. Hamilton, G. P. Asner, C. B. Field, and Ackerly, D. D. The velocity of climate
660 change, *Nature*, 462, 1052-1055 (2009).
- 661 Magri, D., and Sadori, L., Late Pleistocene and Holocene pollen stratigraphy at Lago di Vico, central
662 Italy, *Veg. Hist. .Archaeobot.*, 8, 247-260 (1999).
- 663 Margari, V., Gibbard, P. L., Bryant, C. L., and Tzedakis, P. C., Character of vegetational and
664 environmental changes in southern Europe during the last glacial period; evidence from Lesvos
665 Island, Greece, *Quaternary Sci. Rev.*, 28, 1317-1339 (2009).
- 666 Martinson, D. G., N. G. Pisias, J. D. Hays, J. Imbrie, T. C. Moore, and Shackleton, N. J. Age dating and
667 orbital theory of the Ice Ages: Development of a high-resolution 0 to 300,000-year
668 chronostratigraphy., *Quaternary Res.*, 27, 1-29 (1987).
- 669 Marzin, C., and Braconnot, P., Variations of Indian and African monsoons induced by insolation
670 changes at 6 and 9.5 kyr BP, *Clim. Dyn.*, 33, 215-231 (2009).
- 671 McManus, J. F., Bond, G. C., Broecker, W. S., Johnsen, S., Labeyrie, L. and Higgins, S. High-resolution
672 climate records from the North Atlantic during the last interglacial, *Nature*, 371, 326-329 (1994).
- 673 Nakagawa, T., Gotanda, K., Haraguchi, T., Danhara, T., Yonenobu, H., Brauer, A., Yokoyama, Y., Tada,
674 R., Takemura, K., Staff, R. A., Payne, R., Bronk Ramsey, C., Bryant, C., Brock, F., Schlolaut, G., Marshall,
675 M., Tarasov, P., Lamb, H., SG06, a fully continuous and varved sediment core from Lake Suigetsu,
676 Japan: stratigraphy and potential for improving the radiocarbon calibration model and understanding
677 of late Quaternary climate changes, *Quaternary Sci. Rev.*, 36, 164-176 (2012).
- 678 Newnham, R. M., Eden, D. N., Lowe, D. J. and Hendy, C. H., Rerewhakaaitu Tephra, a land–sea marker
679 for the Last Termination in New Zealand, with implications for global climate change, *Quaternary Sci.
680 Rev.*, 22, 289-308 (2003).
- 681 Ordoñez, A., and Williams, J. W., Climatic and biotic velocities for woody taxa distributions over the
682 last 16 000 years in eastern North America, *Ecol. Lett.*, 16, 773-781 (2013).
- 683 Parnell, A. C., Haslett, J., Allen, J. R. M., Buck, C. E. and Huntley, B. A new approach to assessing
684 synchronicity of past events using Bayesian reconstructions of sedimentation history, *Quaternary Sci.
685 Rev.*, 27, 1872-1885 (2008).
- 686 Prentice, I.C., Records of vegetation in time and space: the principles of pollen analysis. In B. Huntley
687 and T. Webb III (eds), *Vegetation History*, Kluwer, Dordrecht, 17-42 (1988).



- 688 Rasmussen, S. O., Andersen, K. K., Svensson, A., Steffensen, J. P., Vinther, B. M., Clausen, H. B.,
689 Siggaard-Andersen, M.-L., Johnsen, J., Larsen, L. B., Dahl, S. O., Bigler, M., Röthlisberger, R., Fischer,
690 H., Goto-Azuma, K., Hansson, M. E., Ruth, U., A new Greenland ice core chronology for the last glacial
691 termination, *J. Geophys. Res.*, 111 (2006).
- 692 Reille, M., Andrieu, V., de Beaulieu, J.-L., Guenet, P. and Goeury, C., A long pollen record from Lac du
693 Bouchet, Massif Central, France: for the period ca. 325 to 100 ka BP (OIS 9c to OIS 5e), *Quaternary*
694 *Sci. Rev.*, 17, 1107-1123 (1998).
- 695 Reimer, P. J., Bard, E., Bayliss, A., Beck, J. W., Blackwell, P. G., Bronk Ramsey, C., Buck, C. E., Cheng, H.
696 Edwards, R. L. and Friedrich, M., IntCal13 and Marine13 radiocarbon age calibration curves 0-50,000
697 years cal BP (2013).
- 698 Roucoux, K. H., Shackleton, N. J., de Abreu, L., Schönfeld, J. and Tzedakis P. C., Combined marine
699 proxy and pollen analyses reveal rapid Iberian vegetation response to North Atlantic millennial-scale
700 climate oscillations, *Quaternary Res.*, 56, 128-132 (2001).
- 701 Rucina, S. M., Muiruri, V. M., Kinyanjui, R. N., McGuinness, K. and Marchant, R. Late Quaternary
702 vegetation and fire dynamics on Mount Kenya, *Palaeogeogr. Palaeoclimatol.*, 283, 1-14 (2009).
- 703 Sanchez Goñi, M. F., Bard, E., Landais, A., Rossignol, L. and d'Errico, F. Air-sea temperature
704 decoupling in western Europe during the last interglacial-glacial transition, *Nature Geoscience*, 6,
705 837-841 (2013).
- 706 Sanchez Goñi, M. F., Landais, A., Fletcher, W. J., Naughton, F., Desprat, S. and Duprat, J. Contrasting
707 impacts of Dansgaard-Oeschger events over a western European latitudinal transect modulated by
708 orbital parameters, *Quaternary Sci. Rev.*, 27, 1136-1151 (2008).
- 709 Sánchez Goñi, M. F., Introduction to climate and vegetation in Europe during MIS 5, in *The climate of*
710 *past interglacials*, edited by F. Sirocko, Claussen, M., Sánchez Goñi, M.F., Litt, T., pp. 197-205,
711 Elsevier, Amsterdam (2007).
- 712 Sánchez Goñi, M. F., F. Eynaud, J.-L. Turon, and Shackleton, N. J., High resolution palynological record
713 off the Iberian margin: direct land-sea correlation for the Last Interglacial complex, *Earth Planet. Sci.*
714 *Lett.*, 171, 123-137 (1999).
- 715 Sánchez Goñi, M. F., Turon, J.-L., Eynaud, F. and Gendreau, S., European climatic response to
716 millennial-scale climatic changes in the atmosphere-ocean system during the Last Glacial period,
717 *Quaternary Res.*, 54, 394-403 (2000).
- 718 Sawada, K., Arita, Y., Nakamura, T., Akiyama, M., Kamei, T. and Nakai, N., 14C dating of the Nojiri-ko
719 Formation using accelerator mass spectrometry, *Earth Science [Chikyu Kagaku]*, 46, 133-142 (1992).
- 720 Shackleton, N. J., Hall, M. A. and Vincent, E., Phase relationships between millennial scale events
721 64,000-24,000 years ago, *Paleoceanography*, 15, 565-569 (2000).
- 722 Shackleton, N. J., Fairbanks, R. G., Chiu, T. and Parrenin, F., Absolute calibration of the Greenland
723 time scale: implications for Antarctic time scales and for $\Delta^{14}C$, *Quaternary Sci. Rev.*, 23, 1513-1523
724 (2004).



- 725 Shane, P., Smith, V. C., Lowe, D. J. and Nairn, I., Re-identification of c. 15 700 cal yr BP tephra bed at
726 Kaipo Bog, eastern North Island: implications for dispersal of Rotorua and Puketarata tephra beds,
727 *New Zeal. J. Geol. Geop.*, 46, 591-596 (2003).
- 728 Smith, V. C., Staff, R. A., Blockley, S. P. E., Bronk Ramsey, C., Nakagawa, T., Mark, D. F., Takemura, K.
729 and Danhara, T., Identification and correlation of visible tephras in the Lake Suigetsu SG06
730 sedimentary archive, Japan: chronostratigraphic markers for synchronising of east Asian/west Pacific
731 palaeoclimatic records across the last 150 ka, *Quaternary Sci. Rev.*, 67, 121-137 (2013).
- 732 Smith, V. C., Mark, D. F., Staff, R. A., Blockley, S. P. E., Ramsey, C. B., Bryant, C. L., Nakagawa, T., Han,
733 K. K., Weh, A., Takemura, K., Danhara, T., Toward establishing precise $^{40}\text{Ar}/^{39}\text{Ar}$ chronologies for
734 Late Pleistocene palaeoclimate archives: an example from the Lake Suigetsu (Japan) sedimentary
735 record, *Quaternary Sci. Rev.*, 30, 2845-2850 (2011).
- 736 Steffensen, J. P., Andersen, K.K., Bigler, M., Clausen, H.B., Dahl-Jensen, D., Fischer, H., Goto-Azuma,
737 K., Hansson, M., Johnsen, S.J., Jouzel, J., Masson-Delmotte, V., Popp, T., Rasmussen, S.O.,
738 Röthlisberger, R., Ruth, U., Stauffer, B., Siggaard-Andersen, M.-L., Sveinbjörnsdóttir, A.-E., Svensson,
739 A., White, J.W.C., High-Resolution Greenland Ice Core Data Show Abrupt Climate Change Happens in
740 Few Years, *Nature*, 321, 680-684 (2008).
- 741 Svensson, A., Andersen, K.K., Bigler, B., Clausen, H.B., Dahl-Jensen, D., Davies, S.M., Johnsen, S.J.,
742 Muscheler, R., Rasmussen, S.O., Röthlisberger, R., Steffensen, J.P., Vinther, B.M., The Greenland Ice
743 Core Chronology 2005, 15-42 ka. Part 2: comparison to other records, *Quaternary Sci. Rev.* 25, 3258-
744 3267 (2006).
- 745 Svensson, A., Andersen, K. K., Bigler, M., Clausen, H. B., Dahl-Jensen, D., Davies, S. M., Johnsen, S. J.,
746 Muscheler, R., Parrenin, F., Rasmussen, S. O., Röthlisberger, R., Seierstad, I., Steffensen, J. P., Vinther,
747 B. M., A 60 000 year Greenland stratigraphic ice core chronology, *Clim. Past*, 4, 47-57 (2008).
- 748 Takahara, H., Igarashi, Y., Hayashi, R., Kumon, F., Liew, P.-M., Yamamoto, M., Kawai, S., Oba, T. and
749 Irino, T., Millennial-scale variability in vegetation records from the East Asian Islands: Taiwan, Japan
750 and Sakhalin, *Quaternary Sci. Rev.*, 29, 2900-291 (2010)7.
- 751 R Development Core Team, R: A language and environment for statistical computing, in R Foundation
752 for Statistical Computing, edited, Vienna, Austria (2016).
- 753 Tzedakis, P. C., Pälike, H., Roucoux, K. H. and de Abreu, L. Atmospheric methane, southern European
754 vegetation and low-mid latitude links on orbital and millennial timescales, *Earth Planet. Sci. Lett.*,
755 277, 307-317 (2009).
- 756 Vandergoes, M. J., Hogg, A. G., Lowe, D. J., Newnham, R. M., Denton, G. H., Southon, J.R., Barrell, D. J.
757 A., Wilson, C. J. N., McGlone, M. S., Allan, A. S. R., Almond, P. C., Petchey, F., Dabell, K.,
758 Dieffenbacher-Krall, A. C., Blaauw, M., A revised age for the Kawakawa/Oruanui tephra, a key marker
759 for the Last Glacial Maximum in New Zealand, *Quaternary Sci. Rev.*, 74, 195-201 (2013).
- 760 Wang, Y. J., Cheng, H., Edwards, R. L., An, Z. S., Wu, J. Y., Shen, C.-C. and Dorale, J. A. A high-
761 resolution absolute-dated Late Pleistocene monsoon record from Hulu Cave, China, *Science*, 294,
762 2345 (2001).



- 763 Weirauch, D., Billups, K. and Martin (2008), P., Evolution of millennial-scale climate variability during
764 the mid-Pleistocene, *Paleoceanography*, 23, PA3216.
- 765 Whitlock, C., Sarna-Wojcicki, A. M., Bartlein, P. J. and Nickmann, R. J. Environmental history and
766 tephrostratigraphy at Carp Lake, southwestern Columbia Basin, Washington, USA, *Palaeogeogr.*
767 *Palaeocl.*, 155, 7-29 (2000).
- 768 Wolff, E. W., Chappellaz, J., Blunier, T., Rasmussen, S. O. and Svensson, A. C. Millennial-scale
769 variability during the last glacial: The ice core record, *Quaternary Sci. Rev.*, 29, 2828-2838 (2010).
- 770 Wulf, S., Kraml, M., Brauer, A., Keller, J. and Negendan, J. F. W. Tephrochronology of the 100 ka
771 lacustrine sediment record of Lago Grande di Monticchio (southern Italy), *Quatern. Int.*, 122, 7-30
772 (2004).
- 773